

Wavelets for the fast solution of boundary integral equations

Helmut Harbrecht

Fakultät für Mathematik
Technische Universität Chemnitz, 09107 Chemnitz, Germany
e-mail: helmut.harbrecht@mathematik.tu-chemnitz.de

Reinhold Schneider*

Fakultät für Mathematik
Technische Universität Chemnitz, 09107 Chemnitz, Germany
e-mail: reinhold.schneider@mathematik.tu-chemnitz.de

Key words: boundary integral equations, boundary element method, wavelet bases, matrix compression

Abstract

This paper presents a wavelet Galerkin scheme for the fast solution of boundary integral equations. Wavelet Galerkin schemes employ appropriate wavelet bases for the discretization of boundary integral operators. This yields quasi-sparse system matrices which can be compressed to $\mathcal{O}(N_J)$ relevant matrix entries without compromising the accuracy of the underlying Galerkin scheme. Herein, $\mathcal{O}(N_J)$ denotes the number of unknowns. The assembly of the compressed system matrix can be performed in $\mathcal{O}(N_J)$ operations. Therefore, we arrive at an algorithm which solves boundary integral equations within optimal complexity. By numerical experiments we provide results which corroborate the theory.

1 Introduction

Various problems in science and engineering can be formulated as boundary integral equations. In general, boundary integral equations are solved numerically by the boundary element method (BEM). For example, BEM is a favourable approach for the treatment of exterior boundary value problems. Nevertheless, traditional discretizations of integral equations suffer from a major disadvantage. The associated system matrices are densely populated. Therefore, the complexity for solving such equations is at least $\mathcal{O}(N_J^2)$, where N_J denotes the number of equations. This fact restricts the maximal size of the linear equations seriously.

Modern methods for the fast solution of BEM reduce the complexity to a suboptimal rate, i.e., $\mathcal{O}(N_J \log^\alpha N_J)$, or even an optimal rate, i.e., $\mathcal{O}(N_J)$. Prominent examples for such methods are the *fast multipole method* [16], the *panel clustering* [19] or *hierarchical matrices* [18, 30]. As introduced by [1] and improved in [9, 10, 11, 12, 28], wavelet bases offer a further tool for the fast solution of integral equations. In fact, a Galerkin discretization with wavelet bases results in quasi-sparse matrices, i.e., the most matrix entries are negligible and can be treated as zero. Discarding these nonrelevant matrix entries is called matrix compression. It has been shown in [28] that only $\mathcal{O}(N_J)$ significant matrix entries remain.

Concerning boundary integral equations, a strong effort has been spent on the construction of appropriate wavelet bases on surfaces [7, 13, 14, 20, 25, 28]. In order to achieve the optimal complexity of the wavelet Galerkin scheme, wavelet bases are required with a sufficiently large number of vanishing moments. Our realization is based on biorthogonal spline wavelets derived from the multiresolution developed in [4]. These wavelets are advantageous since the regularity of the duals is known [31]. Moreover, the duals are compactly supported which preserves the linear complexity of the fast wavelet transform also for its inverse. This is an important task for the coupling of FEM and BEM, cf. [21, 22]. Additionally, in view of the discretization of operators of positive order, for instance, the hypersingular operator, globally continuous wavelets are available [2, 5, 13, 20].

The efficient computation of the relevant matrix coefficients turned out to be an important task for the successful application of the wavelet Galerkin method [20, 26, 28]. We present a fully discrete Galerkin scheme based on numerical quadrature. Supposing that the given manifold is piecewise analytic we can use a *hp*-quadrature scheme [20, 28, 29] in combination with exponentially convergent quadrature rules. This yields an algorithm with asymptotically linear complexity without compromising the accuracy of the Galerkin scheme.

The outline of the present paper is as follows. First, we introduce the class of problems under consideration. Then, in Section 3 we provide suitable wavelet bases on manifolds. With such bases at hand we are able to introduce the fully discrete wavelet Galerkin scheme in Section 4. We survey on several practical issues like setting up the compression pattern, assembling the system matrix and preconditioning. In Section 5 we present numerical results which confirm our analysis quite well. The accuracy of the Galerkin scheme is never compromised by the matrix compression.

2 Setting up the Problem

For the numerical approximation of a boundary integral equation we need a discretization method which ends up with a sufficiently accurate finite-dimensional approximation of the given operator. At first we

consider a general setting for the boundary element method. Next, a short description of the representation of the geometry on a computer is given. Then, we discuss the properties for the class of kernel functions under consideration.

2.1 Boundary integral equations

We consider a boundary integral equation on the closed boundary surface Γ of a $(n + 1)$ -dimensional domain Ω

$$(\mathcal{A}\rho)(\mathbf{x}) = \int_{\Gamma} k(\mathbf{x}, \mathbf{y})\rho(\mathbf{y})d\sigma_{\mathbf{y}} = f(\mathbf{x}), \quad \mathbf{x} \in \Gamma. \quad (1)$$

Herein, the boundary integral operator \mathcal{A} denotes an operator of the order $2q$, that is $\mathcal{A} : H^q(\Gamma) \rightarrow H^{-q}(\Gamma)$. Especially we are interested in the case $n = 2$.

For the present purpose, we assume that the boundary $\Gamma \in \mathbb{R}^{n+1}$ is represented by piecewise parametric mappings, see Subsection 2.2 for details. The number of different mappings, which is the number of surface patches, will be denoted by M . The surface representation is in contrast to the usual approximation of the surface by panels. It has the advantage that the rate of convergence is not limited by this approximation. Notice that technical surfaces generated by CAD tools are represented in this form. Of course, this fact makes the use of numerical integration indispensable for the computation of the system matrices.

The properties of the class of kernel functions $k(\mathbf{x}, \mathbf{y})$ which are under consideration will be outlined in Subsection 2.3.

2.2 Parametric representation of manifolds

Let \square denote the unit n -cube, i.e., $\square = [0, 1]^n$. We subdivide the given manifold $\Gamma \in \mathbb{R}^{n+1}$ into several *patches*

$$\Gamma = \bigcup_{i=1}^M \Gamma_i, \quad \Gamma_i = \gamma_i(\square), \quad i = 1, 2, \dots, M,$$

such that each $\gamma_i : \square \rightarrow \Gamma_i$ defines a diffeomorphism of \square onto Γ_i . The intersection $\Gamma_i \cap \Gamma_{i'}$, $i \neq i'$, of the patches Γ_i and $\Gamma_{i'}$ is supposed to be either \emptyset or a lower dimensional face. On the level j , the unit cube is subdivided equidistantly j times into 2^{jn} cubes $C_{j,\mathbf{k}} \subseteq \square$, where $\mathbf{k} = (k_1, \dots, k_n)$ with $0 \leq k_m < 2^j$. This yields $2^{jn}M$ elements (or elementary domains) $\Gamma_{i,j,\mathbf{k}} := \gamma_i(C_{j,\mathbf{k}}) \subseteq \Gamma_i$, $i = 1, 2, \dots, M$. In order to get a regular mesh of Γ the parametric representation is subjected to the following matching condition. For all $\mathbf{x} \in \Gamma_i \cap \Gamma_{i'}$ exists a bijective, affine mapping $\Xi : \square \rightarrow \square$ such that $\gamma_i(\mathbf{s}) = (\gamma_{i'} \circ \Xi)(\mathbf{s}) = \mathbf{x}$ for $\mathbf{s} = [s_1, \dots, s_n]^T \in \square$ with $\gamma_i(\mathbf{s}) = \mathbf{x}$, cf. Fig. 1.

The first fundamental tensor of differential geometry is given by the matrix $\mathbf{K}_i(\mathbf{s}) \in \mathbb{R}^{n \times n}$ with

$$\mathbf{K}_i(\mathbf{s}) := \left[\left(\frac{\partial \gamma_i(\mathbf{s})}{\partial s_j}, \frac{\partial \gamma_i(\mathbf{s})}{\partial s_{j'}} \right)_{l^2(\mathbb{R}^{n+1})} \right]_{j,j'=1,\dots,n}.$$

Since γ_i is supposed to be a diffeomorphism, the matrix $\mathbf{K}_i(\mathbf{s})$ is symmetric and positive definite. The canonical inner product in $L^2(\Gamma)$ is given by

$$(u, v)_{L^2(\Gamma)} = \int_{\Gamma} u(\mathbf{x})v(\mathbf{x})d\sigma_{\mathbf{x}} = \sum_{i=1}^M \int_{\square} u(\gamma_i(\mathbf{s}))v(\gamma_i(\mathbf{s}))\sqrt{\det(\mathbf{K}_i(\mathbf{s}))}ds.$$

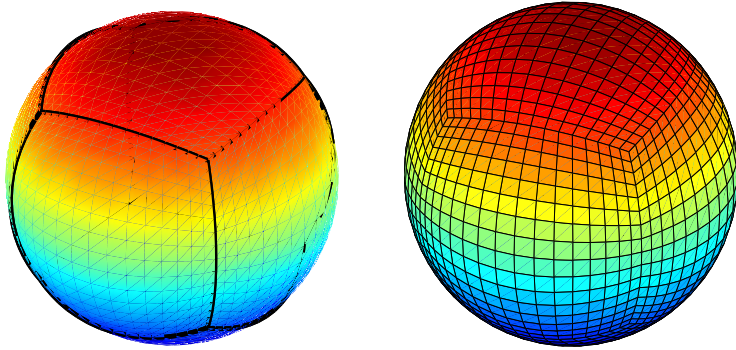


Figure 1: The parametrization of the unit sphere is obtained by projecting it onto the cube $[-1, 1]^3$, which yields six patches (left). On the right hand side one figures out the partition on the level $j = 4$.

The corresponding Sobolev spaces are indicated by $H^s(\Gamma)$. Of course, depending on the global smoothness of the surface, the range of permitted $s \in \mathbb{R}$ is limited to $s \in (-s_\Gamma, s_\Gamma)$.

2.3 Kernel Functions and their Properties

We can now specify the kernel functions. To this end, we denote by $\alpha = (\alpha_1, \dots, \alpha_n)$ and $\beta = (\beta_1, \dots, \beta_n)$ multi-indices of dimension n and define $|\alpha| := \alpha_1 + \dots + \alpha_n$. Moreover, we denote by $k_{i,i'}(\mathbf{s}, \mathbf{t})$ the transported kernel functions, that is

$$k_{i,i'}(\mathbf{s}, \mathbf{t}) := k(\gamma_i(\mathbf{s}), \gamma_{i'}(\mathbf{t})) \sqrt{\det(\mathbf{K}_i(\mathbf{s}))} \sqrt{\det(\mathbf{K}_{i'}(\mathbf{t}))}, \quad 1 \leq i, i' \leq M. \quad (2)$$

Definition 2.1. A kernel $k(\mathbf{x}, \mathbf{y})$ is called standard kernel of the order $2q$, if the partial derivatives of the transported kernel functions $k_{i,i'}(\mathbf{s}, \mathbf{t})$, $1 \leq i, i' \leq M$, are bounded by

$$|\partial_{\mathbf{s}}^\alpha \partial_{\mathbf{t}}^\beta k_{i,i'}(\mathbf{s}, \mathbf{t})| \leq c_{\alpha,\beta} \|\gamma_i(\mathbf{s}) - \gamma_{i'}(\mathbf{t})\|^{-(n+2q+|\alpha|+|\beta|)}$$

provided that $n + 2q + |\alpha| + |\beta| > 0$.

We emphasize that this definition requires patchwise smoothness but *not* global smoothness of the geometry. The surface itself needs to be only Lipschitz. Generally, under this assumption, the kernel of a boundary integral operator \mathcal{A} of order $2q$ is standard of order $2q$. Hence, we may assume this property in the sequel.

3 Wavelets and multiresolution analysis

Multiresolution is by now a well-studied topic in signal processing. There are many excellent accounts about it, we refer the reader to the survey paper [6] and the references therein. Here we collect only some facts which are useful for our purpose.

In general, a multiresolution analysis consists of a nested family of finite dimensional subspaces

$$V_{j_0} \subset V_{j_0+1} \subset \cdots \subset V_j \subset V_{j+1} \cdots \subset \cdots \subset L^2(\Gamma),$$

such that $\dim V_j \sim 2^{jn}$ and

$$\overline{\bigcup_{j \geq j_0} V_j} = L^2(\Gamma).$$

Each space V_j is defined by a single-scale basis $\Phi_j = \{\phi_{j,\mathbf{k}} : \mathbf{k} \in \Delta_j\}$, i.e., $V_j = \text{span } \Phi_j$, where Δ_j denotes a suitable index set with cardinality $|\Delta_j| \sim 2^{nj}$. A final requirement is that these bases are uniformly stable, i.e., for any vector $\mathbf{c} \in l^2(\Delta_j)$ holds

$$\|\mathbf{c}\|_{l^2(\Delta_j)} \sim \|\Phi_j \mathbf{c}\|_{L^2(\Gamma)}$$

uniformly in j . Furthermore, the single-scale bases satisfy a locality condition

$$\text{diam supp } \phi_{j,\mathbf{k}} \sim 2^{-j}.$$

If one is going to use the spaces V_j as trial spaces for the Galerkin scheme then additional properties are required. The trial spaces shall have (*approximation*) *order* $d \in \mathbb{N}$ and *regularity* $\gamma > 0$, that is

$$\begin{aligned} \gamma &= \sup\{s \in \mathbb{R} : V_j \subset H^s(\Gamma)\}, \\ d &= \sup\{s \in \mathbb{R} : \inf_{v_j \in V_j} \|v - v_j\|_0 \lesssim 2^{-js} \|v\|_s\}. \end{aligned}$$

Instead of using only a single-scale j the idea of wavelet concepts is to keep track to increment of information between two adjacent scales j and $j+1$. Since $V_j \subset V_{j+1}$ one decomposes $V_{j+1} = V_j \oplus W_j$ with some complementary space W_j , $W_j \cap V_j = \{0\}$, not necessarily orthogonal to V_j . Of practical interest are the bases of the complementary spaces W_j in V_{j+1}

$$\Psi_j = \{\psi_{j,\mathbf{k}} : \mathbf{k} \in \nabla_j = \Delta_{j+1} \setminus \Delta_j\}.$$

It is supposed that the collections $\Phi_j \cup \Psi_j$ are also uniformly stable bases of V_{j+1} . If

$$\Psi = \bigcup_{j=j_0-1}^{\infty} \Psi_j,$$

where $\Psi_{j_0-1} := \Phi_{j_0}$, is a Riesz-basis of $L_2(\Gamma)$ we will call it a wavelet basis. We assume that these basis functions $\psi_{j,\mathbf{k}}$ are local with respect to the corresponding scale j , i.e.,

$$\text{diam supp } \psi_{j,\mathbf{k}} \sim 2^{-j}$$

and we will normalize them such that $\|\psi_{j,\mathbf{k}}\|_{L_2(\Gamma)} \sim 1$.

We note that at first glance it would be very convenient to deal with a single orthonormal system of wavelets. But it was shown in [12, 28] that orthogonal wavelets are not completely appropriate for the efficient solution of boundary integral equations. For that reason we use biorthogonal wavelet bases. Then, we have also a biorthogonal, or dual, multiresolution analysis, i.e., dual single-scale bases $\tilde{\Phi}_j = \{\tilde{\phi}_{j,\mathbf{k}} : \mathbf{k} \in \Delta_j\}$ and wavelets $\tilde{\Psi}_j = \{\tilde{\psi}_{j,\mathbf{k}} : \mathbf{k} \in \Delta_j\}$ which are coupled to the primal ones via

$$(\Phi_j, \tilde{\Phi}_j)_{L^2(\Gamma)} = \mathbf{I}, \quad (\Psi_j, \tilde{\Psi}_j)_{L^2(\Gamma)} = \mathbf{I}.$$

The associated spaces $\tilde{V}_j := \text{span } \tilde{\Phi}_j$ and $\tilde{W}_j := \text{span } \tilde{\Psi}_j$ satisfy

$$V_j \perp \tilde{W}_j, \quad \tilde{V}_j \perp W_j. \quad (3)$$

Also the dual spaces shall have some order $\tilde{d} \in \mathbb{N}$ and regularity $\tilde{\gamma} > 0$.

Denoting likewise to the primal side

$$\tilde{\Psi} = \bigcup_{j=j_0-1}^{\infty} \tilde{\Psi}_j, \quad \tilde{\Psi}_{j_0-1} := \tilde{\Phi}_{j_0},$$

then, every $v \in L^2(\Gamma)$ has a representation

$$v = \tilde{\Psi}(v, \Psi)_{L^2(\Gamma)} = \Psi(v, \tilde{\Psi})_{L^2(\Gamma)}$$

Moreover, there hold the well known norm equivalences

$$\begin{aligned} \|v\|_t^2 &\sim \sum_{j=j_0-1}^{\infty} 2^{2jt} \|(v, \tilde{\Psi}_j)_{L^2(\Gamma)}\|_{l^2(\nabla_j)}^2, \quad t \in (-\tilde{\gamma}, \gamma), \\ \|v\|_t^2 &\sim \sum_{j=j_0-1}^{\infty} 2^{2jt} \|(v, \Psi_j)_{L^2(\Gamma)}\|_{l^2(\nabla_j)}^2, \quad t \in (-\gamma, \tilde{\gamma}). \end{aligned} \quad (4)$$

The relation (3) implies that the wavelets provide *vanishing moments* or a *cancellation property*

$$|(v, \psi_{j,\mathbf{k}})_{L^2(\Gamma)}| \lesssim 2^{-j(\tilde{d}+n/2)} |v|_{W^{\tilde{d},\infty}(\text{supp } \psi_{j,\mathbf{k}})}. \quad (5)$$

Here $|v|_{W^{\tilde{d},\infty}(\Omega)} := \sup_{|\alpha|=\tilde{d}, x \in \Omega} |\partial^\alpha v(x)|$ denotes the semi-norm in $W^{\tilde{d},\infty}(\Omega)$. We refer to [6] for further details.

For the current type of boundary surfaces Γ the $\Phi_j, \tilde{\Phi}_j$ are generated by constructing first dual pairs of single-scale bases on the interval $[0, 1]$, using B-splines for the primal bases and the dual components from [4] adapted to the interval [8]. Tensor products yield corresponding dual pairs on \square . Using the parametric liftings γ_i and gluing across patch boundaries leads to globally continuous single-scale bases $\Phi_j, \tilde{\Phi}_j$ on Γ , [2, 5, 13, 20]. For B-splines of order d and duals of order $\tilde{d} \geq d$ such that $d + \tilde{d}$ is even the $\Phi_j, \tilde{\Phi}_j$ have approximation orders d, \tilde{d} , respectively. It is known that the respective regularity indices $\gamma, \tilde{\gamma}$ (inside each patch) satisfy $\gamma = d - 1/2$ while $\tilde{\gamma} > 0$ is known to increase proportionally to \tilde{d} . Appropriate wavelet bases are constructed by projecting a *stable completion* into the correct complement spaces (see [3, 13, 28] for details).

4 The Wavelet Galerkin scheme

This section presents a fully discrete wavelet Galerkin scheme for boundary integral equations. In the first subsection we discretize the given boundary integral equation. In Subsection 4.2 we introduce the a-priori matrix compression which reduces the relevant matrix coefficients to an asymptotically linear number. Then, in Subsection 4.3 and Subsection 4.4 we point out the computation of the compressed matrix. Next, in Subsection 4.5 we introduce an a-posteriori compression which reduces again the number of matrix coefficients. The last subsection is dedicated to the preconditioning of system matrices which arise from boundary integral operators of nonzero order.

In the sequel, the collection Ψ_J with a capital J denotes the finite wavelet basis in the space V_J , i.e., $\Psi_J := \bigcup_{j=j_0-1}^{J-1} \Psi_j$. Further, $N_J := \dim V_J \sim 2^{Jn}$ indicates the number of unknowns.

4.1 Discretization

The variational formulation of the given boundary integral equation (1) reads

$$\text{seek } \rho \in H^q(\Gamma) : \quad (\mathcal{A}\rho, \eta)_{L^2(\Gamma)} = (f, \eta)_{L^2(\Gamma)} \quad \forall \eta \in H^q(\Gamma). \quad (6)$$

It is well known, that the variational formulation (6) is equivalent to the boundary integral equation (1), see e.g. [17, 24] for details.

For the Galerkin scheme we replace the energy space $H^q(\Gamma)$ in the variational formulation (6) by the finite dimensional spaces V_J introduced in the previous section. Then, we arrive at the problem

$$\text{seek } \rho_J \in V_J : \quad (\mathcal{A}\rho_J, \eta_J)_{L^2(\Gamma)} = (f, \eta_J)_{L^2(\Gamma)} \quad \forall \eta_J \in V_J.$$

Equivalently, due to the finite dimension of V_J , the ansatz $\rho_J = \Psi_J \boldsymbol{\rho}_J^\psi$ together with

$$\mathbf{A}_J^\psi := (\mathcal{A}\Psi_J, \Psi_J)_{L^2(\Gamma)}, \quad \mathbf{f}_J^\psi := (f, \Psi_J)_{L^2(\Gamma)},$$

yields the wavelet Galerkin scheme

$$\mathbf{A}_J^\psi \boldsymbol{\rho}_J^\psi = \mathbf{f}_J^\psi. \quad (7)$$

The system matrix \mathbf{A}_J^ψ is quasi-sparse and might be compressed to $\mathcal{O}(N_J)$ nonzero matrix entries if the wavelets have a sufficiently large number of vanishing moments. The remainder of this paper is devoted to the efficient computation of the system matrix.

Remark 4.1. *Replacing the wavelet basis Ψ_J by the single-scale basis Φ_J yields the traditional single-scale Galerkin scheme*

$$\mathbf{A}_J^\phi \boldsymbol{\rho}_J^\phi = \mathbf{f}_J^\phi,$$

where $\mathbf{A}_J^\phi := (\mathcal{A}\Phi_J, \Phi_J)_{L^2(\Gamma)}$, $\mathbf{f}_J^\phi := (f, \Phi_J)_{L^2(\Gamma)}$ and $\rho_J = \Phi_J \boldsymbol{\rho}_J^\phi$. This scheme is related to the wavelet Galerkin scheme by

$$\mathbf{A}_J^\psi = \mathbf{T}_J \mathbf{A}_J^\phi \mathbf{T}_J^T, \quad \boldsymbol{\mu}_J^\psi = \mathbf{T}_J^{-T} \boldsymbol{\mu}_J^\phi, \quad \mathbf{f}_J^\psi = \mathbf{T}_J \mathbf{f}_J^\phi,$$

where \mathbf{T}_J denotes the wavelet transform. The system matrix \mathbf{A}_J^ϕ is densely populated. Therefore, the costs of solving a given boundary integral equation traditionally in the single-scale basis is at least $\mathcal{O}(N_J^2)$.

4.2 A-priori compression

The discretization of a boundary integral operator $\mathcal{A} : H^q(\Gamma) \rightarrow H^{-q}(\Gamma)$ by wavelets with a sufficiently large number of vanishing moments (5) yields quasi-sparse matrices. In a first compression step all matrix entries, for which the distances of the supports of the corresponding ansatz and test functions are bigger than a level depending cut-off parameter $\mathcal{B}_{j,j'}$, are set to zero. In the second compression step also some of those matrix entries are neglected, for which the corresponding ansatz and test functions have overlapping supports.

First, we introduce the abbreviation

$$\begin{aligned}\Theta_{j,\mathbf{k}} &:= \text{conv hull}(\text{supp } \psi_{j,\mathbf{k}}), \\ \Xi_{j,\mathbf{k}} &:= \text{sing supp } \psi_{j,\mathbf{k}}.\end{aligned}$$

Note that $\Theta_{j,\mathbf{k}}$ denotes the convex hull to the support of $\psi_{j,\mathbf{k}}$ while $\Xi_{j,\mathbf{k}}$ denotes the so-called *singular support* of $\psi_{j,\mathbf{k}}$, i.e., those points where $\psi_{j,\mathbf{k}}$ is not smooth.

The compressed system matrix \mathbf{A}_J^ψ corresponding to the boundary integral operator \mathcal{A} is defined by

$$[\mathbf{A}_J^\psi]_{(j,\mathbf{k}),(j',\mathbf{k}')} := \begin{cases} 0, & \text{dist}(\Theta_{j,\mathbf{k}}, \Theta_{j',\mathbf{k}'}) > \mathcal{B}_{j,j'}, j, j' \geq j_0, \\ 0, & \text{dist}(\Xi_{j,\mathbf{k}}, \Theta_{j',\mathbf{k}'}) > \mathcal{B}'_{j,j'}, j' > j, \\ 0, & \text{dist}(\Theta_{j,\mathbf{k}}, \Xi_{j',\mathbf{k}'}) > \mathcal{B}'_{j,j'}, j > j', \\ (\mathcal{A}\psi_{j',\mathbf{k}'}, \psi_{j,\mathbf{k}})_{L^2(\Gamma)}, & \text{otherwise.} \end{cases} \quad (8)$$

Herein, choosing

$$a, a' > 1, \quad d < \delta, \delta' < \tilde{d} + 2q, \quad (9)$$

the cut-off parameters $\mathcal{B}_{j,j'}$ and $\mathcal{B}'_{j,j'}$ are set as follows

$$\begin{aligned}\mathcal{B}_{j,j'} &= a \max \left\{ 2^{-\min\{j,j'\}}, 2^{\frac{2J(\delta-q)-(j+j')(\delta+\tilde{d})}{2(d+q)}} \right\}, \\ \mathcal{B}'_{j,j'} &= a' \max \left\{ 2^{-\max\{j,j'\}}, 2^{\frac{2J(\delta'-q)-(j+j')\delta' - \max\{j,j'\}\tilde{d}}{\tilde{d}+2q}} \right\}.\end{aligned} \quad (10)$$

The resulting structure of the compressed matrix is figuratively called *finger structure*, cf. Fig. 2. It is shown in [28] that this compression strategy does not compromise the stability and accuracy of the underlying Galerkin scheme.

Theorem 4.2. *Let the system matrix \mathbf{A}_J^ψ be compressed in accordance with (8), (9) and (10). Then, the wavelet Galerkin scheme is stable and the error estimate*

$$\|\rho - \rho_J\|_{H^{2q-d}(\Gamma)} \lesssim 2^{-2J(d-q)} \|\rho\|_{H^d(\Gamma)} \quad (11)$$

holds, where $\rho \in H^d(\Gamma)$ denotes the exact solution of the given boundary integral equation $\mathcal{A}\rho = f$ and $\rho_J = \Psi_J \rho_J^\psi$ is the numerically computed solution, i.e., $\mathbf{A}_J^\psi \rho_J^\psi = \mathbf{f}^\psi$.

The next theorem shows that the over-all complexity of assembling the compressed system matrix is $\mathcal{O}(N_J)$ even if each entry is weighted by a logarithmical penalty term [20]. We mention that the choice $\alpha = 0$ proves that the a-priori compression yields $\mathcal{O}(N_J)$ relevant matrix entries in the compressed system matrix.

Theorem 4.3. *Let the system matrix $\mathbf{A}_J^\psi = (\mathcal{A}\Psi_J, \Psi_J)_{L^2(\Gamma)}$ be compressed according to (8), (9) and (10). The complexity of computing this compressed matrix is $\mathcal{O}(N_J)$ if the calculation of its entries $(\mathcal{A}\psi_{j',\mathbf{k}'}, \psi_{j,\mathbf{k}})_{L^2(\Gamma)}$ is performed in $\mathcal{O}([J - \frac{j+j'}{2}]^\alpha)$ operations with some $\alpha \geq 0$.*

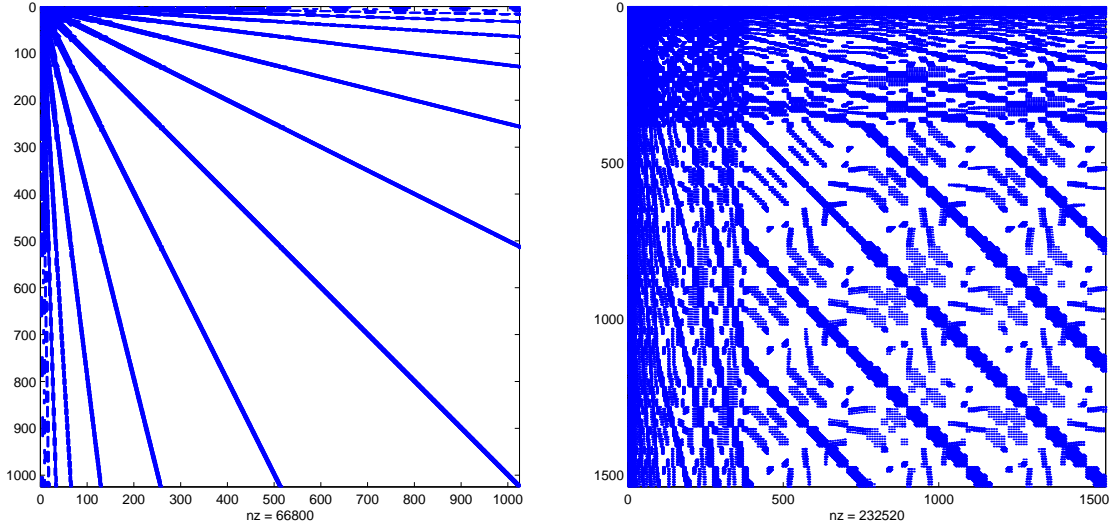


Figure 2: The finger structure of the compressed system matrix computed with respect to the two dimensional (left) and the three dimensional (right) unit spheres.

4.3 Setting up the compression pattern

In order to compute the matrix compression we cannot check the distance criterion (8) for each matrix coefficient since this leads to $\mathcal{O}(N_J^2)$ functions calls. To realize linear complexity, we exploit the underlying tree structure with respect to the supports of the wavelets, to predict negligible matrix coefficients. We will call a wavelet $\psi_{j+1,\text{son}}$ a son of $\psi_{j,\text{father}}$ if $\Theta_{j+1,\text{son}} \subseteq \Theta_{j,\text{father}}$.

Lemma 4.4. *We consider $\Theta_{j+1,\text{son}} \subseteq \Theta_{j,\text{father}}$ and $\Theta_{j'+1,\text{son}} \subseteq \Theta_{j',\text{father}}$.*

1. If

$$\text{dist}(\Theta_{j,\text{father}}, \Theta_{j',\text{father}'}) > \mathcal{B}_{j,j'}$$

then there holds

$$\begin{aligned} \text{dist}(\Theta_{j+1,\text{son}}, \Theta_{j',\text{father}'}) &> \mathcal{B}_{j+1,j'} \\ \text{dist}(\Theta_{j+1,\text{son}}, \Theta_{j'+1,\text{son}'}) &> \mathcal{B}_{j+1,j'+1}. \end{aligned}$$

2. For $j > j'$ suppose

$$\text{dist}(\Theta_{j,\text{father}}, \Xi_{j',\text{father}'}) > \mathcal{B}'_{j,j'}$$

then we can conclude that

$$\text{dist}(\Theta_{j+1,\text{son}}, \Xi_{j',\text{father}'}) > \mathcal{B}'_{j+1,j'}$$

With the help of this lemma we have to check the distance criteria only for coefficients which stem from subdivision of calculated coefficients on a coarser level. Therefore, the resulting procedure of checking the distance criteria is still linear.

4.4 Assembly of the compressed matrix

Up to this point we know that the compressed system matrix has at most $\mathcal{O}(N_J)$ nonzero entries. Now we discuss how to compute the relevant matrix coefficients $(\mathcal{A}\psi_{j',\mathbf{k}'}, \psi_{j,\mathbf{k}})_{L^2(\Gamma)}$ in the Galerkin approach. The matrix entries are given by a double integral over the support of the basis functions, which in the case of a three-dimensional problem is a doubled two-dimensional integration. Unfortunately even for cardinal B-splines it is not possible to determine the matrix entries analytically. Therefore we are forced to compute the matrix coefficients by quadrature rules. This causes an additional error which has to be controlled and it takes place against a background of realizing asymptotically optimal accuracy while preserving efficiency. This means that the numerical methods have to be chosen carefully such that the desired linear complexity of the algorithm is not violated. However, it is not obvious that the complexity in order to compute the relevant coefficients is still linear. It is an immediate consequence of the fact that we require only a level dependent precision of quadrature, cf. [20, 28].

Lemma 4.5. *Let the error of quadrature for computing the relevant matrix coefficients $(\mathcal{A}\psi_{j',\mathbf{k}'}, \psi_{j,\mathbf{k}})_{L^2(\Gamma)}$ be bounded by the level dependent accuracy*

$$\varepsilon_{j,j'} \sim \min \left\{ 2^{-|j-j'|n/2}, 2^{-2n(J-\frac{j+j'}{2})\frac{\delta-q}{d+q}} \right\} 2^{2Jq} 2^{-2d'(J-\frac{j+j'}{2})} \quad (12)$$

with some $d' > d$ and $\delta \in (d, \tilde{d} + r)$ from (9). Then, the Galerkin scheme is stable and converges with the optimal order (11).

From (12) we conclude that the entries on the coarse grids have to be computed with the full accuracy while the entries on the finer grids are allowed to have less accuracy. Unfortunately, the domains of integration are very large on coarser scales.

0	0	0	0	0	0	0	0	0	0	0	0
				$\frac{19}{64}$	$\frac{45}{64}$	$\frac{45}{64}$	$\frac{19}{64}$				
				$\frac{19}{64}$	$\frac{45}{64}$	$\frac{45}{64}$	$\frac{19}{64}$				
0	$\frac{3}{16}$	$\frac{3}{16}$	$\frac{19}{16}$	$\frac{19}{32}$	$\frac{45}{32}$	$\frac{45}{32}$	$\frac{19}{32}$	$\frac{19}{16}$	$\frac{3}{16}$	$\frac{3}{16}$	0
0	$\frac{3}{16}$	$\frac{3}{16}$	$\frac{19}{16}$	$\frac{19}{32}$	$\frac{45}{32}$	$\frac{45}{32}$	$\frac{19}{32}$	$\frac{19}{16}$	$\frac{3}{16}$	$\frac{3}{16}$	0
				$\frac{19}{64}$	$\frac{45}{64}$	$\frac{45}{64}$	$\frac{19}{64}$				
				$\frac{19}{64}$	$\frac{45}{64}$	$\frac{45}{64}$	$\frac{19}{64}$				
0	0	0	0	0	0	0	0	0	0	0	0

Figure 3: The element-based representation of a piecewise linear wavelet with four vanishing moments.

According to the fact that a wavelet is a linear combination of scaling functions the numerical integration can be reduced to interactions of polynomial shape functions on certain elements. This suggests to employ an element-based representation of the wavelets like illustrated in Fig. 3 in the case of a piecewise linear wavelet. Consequently, we have only to deal with integrals of the form

$$I(\Gamma_{i,j,\mathbf{k}}, \Gamma_{i',j',\mathbf{k}'}) := \int_{C_{j,\mathbf{k}}} \int_{C_{j',\mathbf{k}'}} k_{i,i'}(\mathbf{s}, \mathbf{t}) p_l(\mathbf{s}) p_{l'}(\mathbf{t}) d\mathbf{t} d\mathbf{s} \quad (13)$$

with p_l denoting the polynomial shape functions and the transported kernel function (2). This is quite similar to the traditional Galerkin discretization. The main difference is that in the wavelet approach the elements may appear on different levels due to the multilevel hierarchy of wavelet bases.

Difficulties arise if the domains of integration are very close together relatively to their size. We have to apply numerical integration carefully in order to keep the number of evaluations of the kernel function at the quadrature knots moderate and to fulfill the assumptions of Theorem 4.3. In [20, 28, 29] a geometrically graded subdivision is proposed in combination with varying polynomial degrees of approximation in the integration rules, cf. Fig. 4. This provides that the parametric liftings γ_i are analytical. As shown in [20] the combination of tensor product Gauß-Legendre quadrature rules with such a hp -quadrature scheme leads to the number of quadrature points satisfying the assumption of Theorem 4.3 with $\alpha = 2n$.

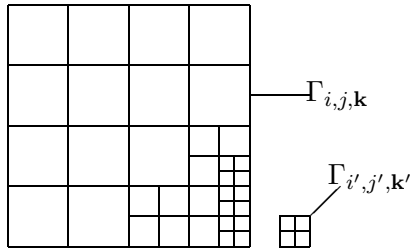


Figure 4: Adaptive subdivision of the domains of integration.

Since the kernel function $k(\mathbf{x}, \mathbf{y})$ has a singularity on the diagonal $\mathbf{x} = \mathbf{y}$, we are confronted with singular integrals if the domains of integration live on the same level and have any points in common. This situation appears if the underlying elements are identical or share a common edge or vertex. Such singular integrals can be treated by the so-called *Duffy-trick* [15, 27], which transform the singular integrands onto analytical ones.

4.5 A-posteriori compression

Let $\mathcal{A} : H^{-q}(\Gamma) \rightarrow H^q(\Gamma)$ be a boundary integral operator and \mathbf{A}_J^ψ the associated system matrix compressed according to Subsection 4.2. If the entries of the compressed system matrix \mathbf{A}_J^ψ have been computed, we may apply an a-posteriori compression by setting all entries to zero, which are smaller than a level depending threshold. That way, a matrix $\tilde{\mathbf{A}}_J^\psi$ is obtained which has less nonzero entries than the matrix \mathbf{A}_J^ψ . Clearly, this does not accelerate the calculation of the matrix coefficients. But the requirement to the memory is reduced if the system matrix has to be stored. For instance, this is advantageous for the coupling of FEM and BEM, cf. [21, 22]. To our experiences this procedure reduces the number of nonzero coefficients by a factor 2–5.

Theorem 4.6. *We define the a-posteriori compression by*

$$[\tilde{\mathbf{A}}_J^\psi]_{(j,\mathbf{k}),(j',\mathbf{k}')} = \begin{cases} 0, & \text{if } |[\mathbf{A}_J^\psi]_{(j,\mathbf{k}),(j',\mathbf{k}')}| \leq \varepsilon_{j,j'}, \\ [\mathbf{A}_J^\psi]_{(j,\mathbf{k}),(j',\mathbf{k}')}, & \text{if } |[\mathbf{A}_J^\psi]_{(j,\mathbf{k}),(j',\mathbf{k}')}| > \varepsilon_{j,j'}. \end{cases}$$

Herein, the level dependent threshold $\varepsilon_{j,j'}$ is chosen as in (12) with some $d' > d$ and $\delta \in (d, \tilde{d} + r)$ from (9). Then, the optimal order of convergence (11) of the Galerkin scheme is not compromised.

4.6 Wavelet preconditioning

Let $\mathcal{A} : H^q(\Gamma) \rightarrow H^{-q}(\Gamma)$ denote a boundary integral operator of the order $2q$ with $q \neq 0$. Then, the corresponding system matrix \mathbf{A}_J^ψ is ill conditioned. In fact, there holds $\text{cond}_{l^2} \mathbf{A}_J^\psi \sim 2^{2J|q|}$. According to [6, 28], the wavelet approach offers a simple diagonal preconditioner based on the norm equivalences.

Theorem 4.7. *Let the diagonal matrix \mathbf{D}_J^r defined by*

$$[\mathbf{D}_J^r]_{(j,k),(j',k')} = 2^{rj} \delta_{j,j'} \delta_{k,k'}, \quad k \in \nabla_j, \quad k' \in \nabla_{j'}, \quad j_0 - 1 \leq j, j' < J. \quad (14)$$

Then, if $\mathcal{A} : H^q(\Gamma) \rightarrow H^{-q}(\Gamma)$ denotes a boundary integral operator of the order $2q$ with $\tilde{\gamma} > -q$, the diagonal matrix \mathbf{D}_J^{2q} defines a preconditioner to \mathbf{A}_J^ψ , i.e.,

$$\text{cond}_{l^2}(\mathbf{D}_J^{-q} \mathbf{A}_J^\psi \mathbf{D}_J^{-q}) \sim 1.$$

Remark 4.8. *The coefficients on the main diagonal of \mathbf{A}_J^ψ satisfy $(\mathcal{A}\psi_{j,k}, \psi_{j,k})_{L^2(\Gamma)} \sim 2^{2qj}$. Therefore, the above preconditioning can be replaced by a diagonal scaling. In fact, the diagonal scaling improves and simplifies the wavelet preconditioning.*

As the numerical results in [23] confirm, this preconditioning works well in the two dimensional case. However, in the three dimensions, the results are not satisfactory. One figures out of Fig. 5 the condition numbers of the stiffness matrices with respect to the single layer operator on a square discretized by piecewise linears. We employed different constructions for wavelets with four vanishing moments (spanning identical spaces, cf. [20] for details). In spite of the preconditioning, the condition numbers with respect to the wavelets are not significantly better than with respect to the single-scale basis. We mention that the situation becomes even worse for operators defined on more complicated geometries.

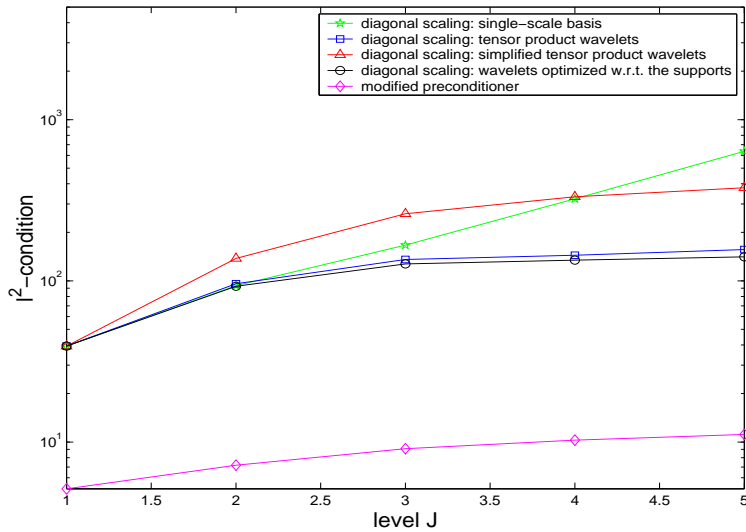


Figure 5: The l^2 -condition numbers with respect to the single layer operator on the unit square and piecewise linear wavelets with four vanishing moments.

A slight modification of the wavelet preconditioner yields much better results. The simple trick is to combine the above preconditioner with the mass matrix which yields an appropriate operator based preconditioning.

Theorem 4.9. *We consider a boundary integral operator $\mathcal{A} : H^q(\Gamma) \rightarrow H^{-q}(\Gamma)$ with corresponding Galerkin matrix \mathbf{A}_J^ψ . Let \mathbf{D}_J^r be defined as in (14) and $\mathbf{B}_J^\psi := (\Psi_J, \Psi_J)_{L^2(\Gamma)}$ denote the mass matrix. Then, if $\tilde{\gamma} > -q$, the matrix $\mathbf{C}_J^{2q} = \mathbf{D}_J^q \mathbf{B}_J^\psi \mathbf{D}_J^q$ defines a preconditioner to \mathbf{A}_J^ψ , i.e.,*

$$\text{cond}_{l^2} \left((\mathbf{C}_J^{2q})^{-1/2} \mathbf{A}_J^\psi (\mathbf{C}_J^{2q})^{-1/2} \right) \sim 1.$$

This preconditioner decreases the condition numbers impressively, cf. Fig. 5. Let us remark that the condition depends on the underlying spaces but not on the chosen wavelet basis. To our experiences the condition reduces about the factor 10–100 compared to the preconditioner (14).

5 Numerical Results

This section is dedicated to numerical examples in order to confirm our theory. Firstly, we compute a Dirichlet problem. We use the indirect formulation for the double layer operator which gives a Fredholm's integral equation of the second kind. This is approximated by using piecewise constant wavelets. Secondly, we solve a Neumann problem employing the indirect formulation for the hypersingular operator. The discretization requires globally continuous piecewise linear wavelets. We mention that both problems are chosen such that the solutions are known analytically in order to measure the error of method.

5.1 Dirichlet Problem

For a given function $f \in H^{1/2}(\Gamma)$ we consider an interior Dirichlet problem, i.e., we seek $u \in H^1(\Omega)$ such that

$$\begin{aligned} \Delta u &= 0 && \text{in } \Omega, \\ u &= f && \text{on } \Gamma. \end{aligned} \tag{15}$$

The domain Ω is described by the set difference of the cube $[-1, 1]^3$ and three cylinders with radii 0.5, cf. Fig. 6. The boundary Γ is parametrized via 48 patches. Choosing the harmonical polynomial

$$u(\mathbf{x}) = 4x^2 - 3y^2 - z^2$$

and setting $f := u|_\Gamma$ the problem (15) has the unique solution u .

We employ the *double layer operator*

$$(\mathcal{K}\rho)(\mathbf{x}) := \frac{1}{4\pi} \int_{\Gamma} \frac{\partial}{\partial \mathbf{n}_{\mathbf{y}}} \frac{1}{\|\mathbf{x} - \mathbf{y}\|^2} \rho(\mathbf{y}) d\sigma_{\mathbf{y}}, \quad \mathbf{x} \in \Gamma, \tag{16}$$

which yields a Fredholm integral equation of the second kind

$$(\mathcal{K} - \frac{1}{2}I)\rho = f \quad \text{on } \Gamma$$

for the unknown density ρ . The solution u of the Dirichlet problem is derived by application of the double layer operator to this density, i.e.,

$$u = \mathcal{K}\rho \quad \text{in } \Omega. \tag{17}$$

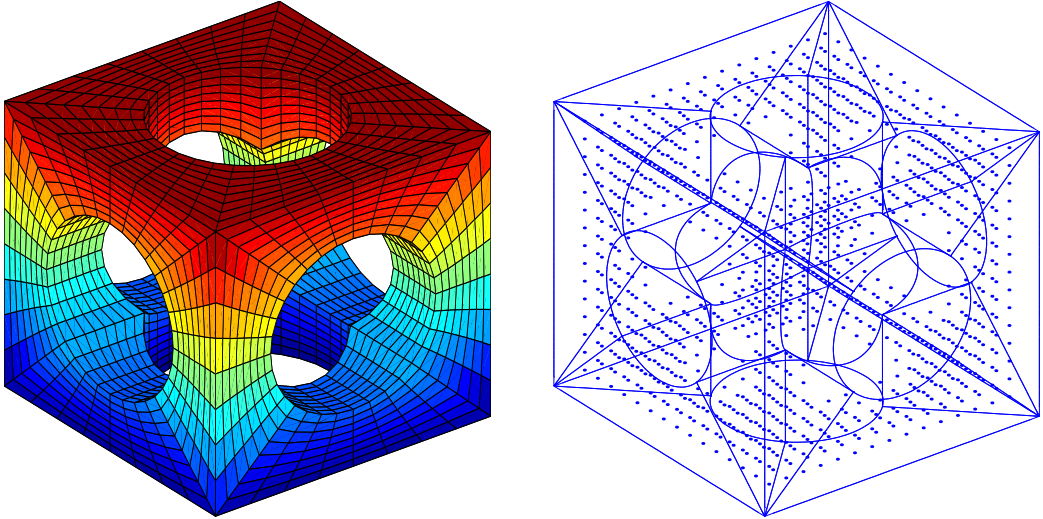


Figure 6: The mesh on the surface Γ and the evaluation points \mathbf{x}_i of the potential.

The operator on the left hand side of (16) defines an operator of the order 0. We discretize this equation by piecewise constant wavelets with three vanishing moments which is in accordance with (9). The discrete solutions are denoted by

$$\mathbf{u} := [u(\mathbf{x}_i)], \quad \mathbf{u}_J^\phi := [(\mathcal{K}\rho_J^\phi)(\mathbf{x}_i)], \quad \mathbf{u}_J^\psi := [(\mathcal{K}\rho_J^\psi)(\mathbf{x}_i)], \quad (18)$$

where the evaluation points \mathbf{x}_i are specified in Fig. 6. Herein, \mathbf{u}_J^ϕ indicates the approximation computed by the traditional Galerkin scheme while \mathbf{u}_J^ψ stands for the numerical solution of the wavelet Galerkin scheme.

In Tab. 1 we list the maximum norm of the absolute errors of \mathbf{u}_J^ϕ and \mathbf{u}_J^ψ . The columns titled by “contr.” (contraction) contain the ratio of the absolute error obtained on the previous level divided by the present absolute error. The optimal order of convergence is quadratic which implies a contraction close to 4. As the results in Tab. 1 confirm, the precisions of the single-scale and the compressed wavelet Galerkin scheme are rather similar.

unknowns		scaling functions $\phi^{(1)}$		wavelets $\psi^{(1,3)}$	
J	N_J	$\ \mathbf{u} - \mathbf{u}_J^\phi\ _\infty$	contr.	$\ \mathbf{u} - \mathbf{u}_J^\psi\ _\infty$	contr.
1	192	1.9	—	2.6	—
2	768	3.3e-1	4.0	4.1e-1	6.2
3	3072	5.7e-2	4.4	6.6e-2	6.2
4	12288	(1.4e-2)	(4.0)	1.3e-2	5.0
5	49152	(3.6e-3)	(4.0)	3.3e-3	4.0

Table 1: The maximum norm of the absolute errors of the discrete potential.

Fig. 7 is concerned with the rates of compression (left) and the computing times (right). We measure the rates of compression by the ratio (in %) of the number of nonzero matrix coefficients and N_J^2 . For $N_J = 49152$ unknowns only 0.78% of the matrix coefficients are relevant. After the a-posteriori compression this

number is even reduced to 0.15%. In the plot on the right hand side of Fig. 7 one finds a comparison of the over-all computing times of the traditional and the fast wavelet discretization. Note that we extrapolated the computing times of the traditional scheme to the levels 4 and 5. For $N_J = 49152$ we obtain the speed-up factor 11.4 in comparison with the single-scale scheme.

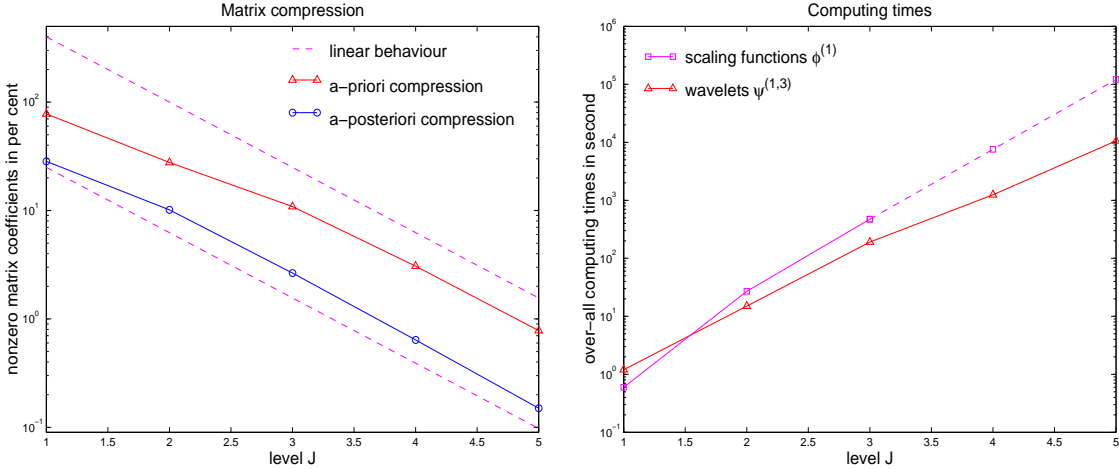


Figure 7: The compression rates and computing times.

5.2 Neumann Problem

For a given function $g \in H^{-1/2}(\Gamma)$ with $\int_{\Gamma} g(\mathbf{x}) d\sigma_{\mathbf{x}} = 0$ we treat a Neumann problem on the domain Ω , that is, we seek $u \in H^1(\Omega)$ such that

$$\begin{aligned} \Delta u &= 0 && \text{in } \Omega, \\ \frac{\partial u}{\partial \mathbf{n}} &= g && \text{on } \Gamma. \end{aligned} \quad (19)$$

The domain Ω under consideration is described as the union of two spheres $B_1([0, 0, \pm 2]^T)$ and one connecting cylinder with the radius 0.5, compare Fig. 8. The boundary Γ is represented via 14 patches. Choosing the harmonical function

$$u(\mathbf{x}) = \frac{(\mathbf{a}, \mathbf{x} - \mathbf{b})}{\|\mathbf{x} - \mathbf{b}\|^3}, \quad \mathbf{a} = [1, 2, 4]^T, \quad \mathbf{b} = [1, 0, 0]^T, \quad (20)$$

and setting $g := \frac{\partial u|_{\Gamma}}{\partial \mathbf{n}}$ the Neumann problem has the solution u modulo a constant.

The *hypersingular operator* \mathcal{W} is given by

$$(\mathcal{W})\rho(\mathbf{x}) := -\frac{1}{4\pi} \frac{\partial}{\partial \mathbf{n}_{\mathbf{x}}} \int_{\Gamma} \frac{\partial}{\partial \mathbf{n}_{\mathbf{y}}} \frac{1}{\|\mathbf{x} - \mathbf{y}\|^2} \rho(\mathbf{y}) d\sigma_{\mathbf{y}}, \quad \mathbf{x} \in \Gamma,$$

and defines an operator of order +1. In order to solve problem (19) we seek the density ρ satisfying the Fredholm integral equation of the first kind

$$\mathcal{W}\rho = g \quad \text{on } \Gamma. \quad (21)$$

Since \mathcal{W} is symmetric and positive semidefinite, cf. [17, 24], one restricts ρ by the constraint $\int_{\Gamma} \rho(\mathbf{x}) d\sigma_{\mathbf{x}} = 0$. We emphasize that the discretization of the hypersingular operator requires *globally*

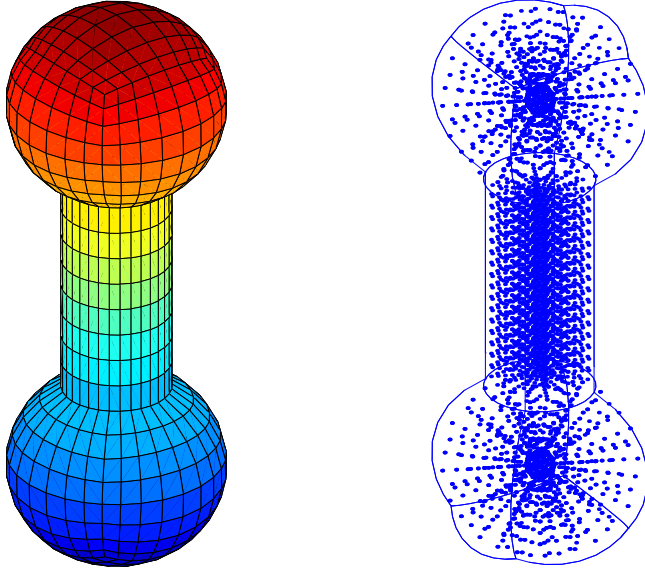


Figure 8: The mesh on the surface Γ and the evaluation points \mathbf{x}_i of the potential.

continuous piecewise linear wavelets. According to (9) piecewise linear wavelets have to provide two vanishing moments.

The density ρ given by the boundary integral equation (21) leads to the solution u of the Neumann problem by application of the double layer operator according to (17). The discrete counterparts are denoted as in (18), where the evaluation points \mathbf{x}_i are specified in Fig. 8.

First, we compare the errors of approximation with respect to the discrete potentials. The order of convergence is cubic (contraction 8) if the density is sufficiently smooth. The results in Tab. 2 suggest even a higher rate of convergence. But asymptotically one expects an order of convergence less than cubic due to concave angles between the patches. The wavelet Galerkin scheme achieves the same accuracy as the traditional Galerkin scheme.

unknowns		scaling functions $\phi^{(2)}$		wavelets $\psi^{(2,2)}$	
J	N_J	$\ \mathbf{u}_J - \mathbf{u}_J^\phi\ _\infty$	contr.	$\ \mathbf{u}_J - \mathbf{u}_J^\psi\ _\infty$	contr.
1	58	7.1	—	7.6	—
2	226	4.3	1.4	4.2	1.8
3	898	1.2	3.6	1.2	3.5
4	3586	1.9e-1	6.3	1.9e-1	6.2
5	14338	(2.4e-2)	(8.0)	1.4e-2	14
6	57346	(3.0e-3)	(8.0)	4.8e-4	30

Table 2: The maximum norm of the absolute errors of the discrete potential.

Next, we visualize again the rates of compression and computing times, see Fig. 9. On the left hand side we plot the number of nonzero coefficients in percent. For $N_J = 57346$ unknowns the matrix compres-

sion yields only 1.37 % and 0.73 % relevant matrix entries after a-priori and a-posteriori compression, respectively. On the right hand side one figures out the over-all computing times. We extrapolated the computing times of the traditional scheme to the levels 5 and 6. On level 6 the speed-up of the wavelet Galerkin scheme is about the factor 11 compared to the traditional scheme.

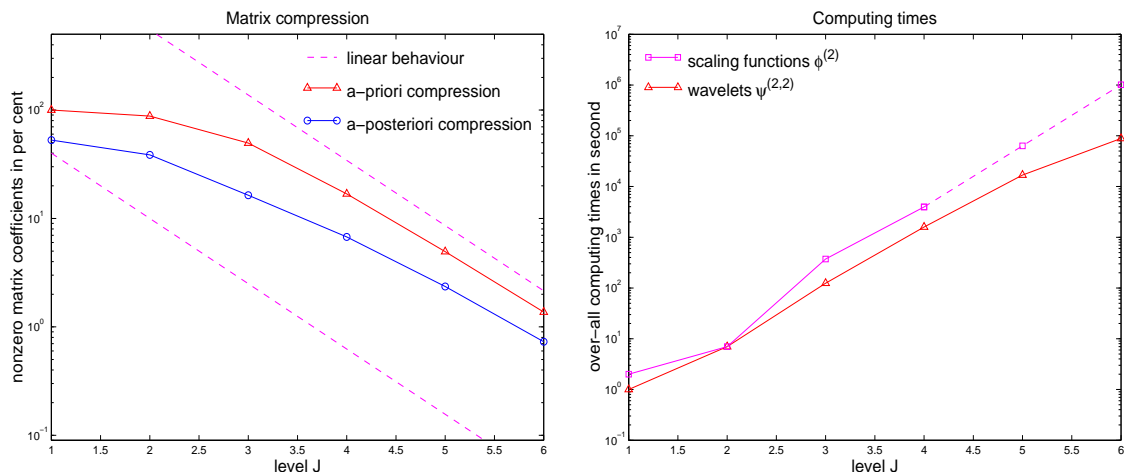


Figure 9: The compression rates and computing times.

References

- [1] G. Beylkin, R. Coifman, and V. Rokhlin. The fast wavelet transform and numerical algorithms. *Comm. Pure and Appl. Math.*, 44:141–183, 1991.
- [2] C. Canuto, A. Tabacco, and K. Urban. The wavelet element method, part I: Construction and analysis. *Appl. Comput. Harm. Anal.*, 6:1–52, 1999.
- [3] J. Carnicer, W. Dahmen, and J. Peña. Local decompositions of refinable spaces. *Appl. Comp. Harm. Anal.*, 3:127–153, 1996.
- [4] A. Cohen, I. Daubechies, and J.-C. Feauveau. Biorthogonal bases of compactly supported wavelets. *Pure Appl. Math.*, 45:485–560, 1992.
- [5] A. Cohen and R. Masson. Wavelet adaptive method for second order elliptic problems – boundary conditions and domain decomposition. *Numer. Math.*, 86:193–238, 2000.
- [6] W. Dahmen. Wavelet and multiscale methods for operator equations. *Acta Numerica*, 6:55–228, 1997.
- [7] W. Dahmen, B. Kleemann, S. Prößdorf, and R. Schneider. A multiscale method for the double layer potential equation on a polyhedron. In H.P. Dikshit and C.A. Micchelli, editors, *Advances in Computational Mathematics*, pages 15–57, World Scientific Publ., Singapore, 1994.
- [8] W. Dahmen, A. Kunoth, and K. Urban. Biorthogonal spline-wavelets on the interval – stability and moment conditions. *Appl. Comp. Harm. Anal.*, 6:259–302, 1999.

- [9] W. Dahmen, S. Prößdorf, and R. Schneider. Multiscale methods for pseudodifferential equations. In L.L. Schumaker and G. Webb, editors, *Wavelet Analysis and its Applications*, volume 3, pages 191–235, 1993.
- [10] W. Dahmen, S. Prößdorf, and R. Schneider. Wavelet approximation methods for periodic pseudodifferential equations. Part II – Fast solution and matrix compression. *Advances in Computational Mathematics*, 1:259–335, 1993.
- [11] W. Dahmen, S. Prößdorf, and R. Schneider. Wavelet approximation methods for periodic pseudodifferential equations. Part I – Convergence analysis. *Mathematische Zeitschrift*, 215:583–620, 1994.
- [12] W. Dahmen, S. Prößdorf, and R. Schneider. Multiscale methods for pseudodifferential equations on smooth manifolds. In C.K. Chui, L. Montefusco, and L. Puccio, editors, *Proceedings of the International Conference on Wavelets: Theory, Algorithms, and Applications*, pages 385–424, 1995.
- [13] W. Dahmen and R. Schneider. Composite wavelet bases for operator equations. *Math. Comp.*, 68:1533–1567, 1999.
- [14] W. Dahmen and R. Schneider. Wavelets on manifolds I. Construction and domain decomposition. *Math. Anal.*, 31:184–230, 1999.
- [15] M. Duffy. Quadrature over a pyramid or cube of integrands with a singularity at the vertex. *SIAM J. Numer. Anal.*, 19:1260–1262, 1982.
- [16] L. Greengard and V. Rokhlin. A fast algorithm for particle simulation. *J. Comput. Phys.*, 73:325–348, 1987.
- [17] W. Hackbusch. *Integralgleichungen*. B.G. Teubner, Stuttgart, 1989.
- [18] W. Hackbusch. A sparse matrix arithmetic based on \mathcal{H} -matrices. Part I: Introduction to \mathcal{H} -matrices. *Computing*, 64:89–108, 1999.
- [19] W. Hackbusch and Z.P. Nowak. On the fast matrix multiplication in the boundary element method by panel clustering. *Numer. Math.*, 54:463–491, 1989.
- [20] H. Harbrecht. Wavelet Galerkin schemes for the boundary element method in three dimensions. *PHD Thesis, Technische Universität Chemnitz, Germany*, 2001.
- [21] H. Harbrecht, F. Paiva, C. Pérez, and R. Schneider. Biorthogonal wavelet approximation for the coupling of FEM-BEM. *Preprint SFB 393/99-32, TU Chemnitz*, 1999. to appear in *Numer. Math.*
- [22] H. Harbrecht, F. Paiva, C. Pérez, and R. Schneider. Wavelet preconditioning for the coupling of FEM-BEM. *Preprint SFB 393/00-07, TU Chemnitz*, 2000. submitted to *Numerical Linear Algebra with Applications*.
- [23] H. Harbrecht and R. Schneider. Wavelet Galerkin Schemes for 2D-BEM. In *Operator Theory: Advances and Applications*, volume 121. Birkhäuser, (2001).
- [24] R. Kress. *Linear Integral Equations*. Springer-Verlag, Berlin-Heidelberg, 1989.

- [25] T. von Petersdorff, R. Schneider, and C. Schwab. Multiwavelets for second kind integral equations. *SIAM J. Num. Anal.*, 34:2212–2227, 1997.
- [26] T. von Petersdorff and C. Schwab. Fully discretized multiscale Galerkin BEM. In W. Dahmen, A. Kurdila, and P. Oswald, editors, *Multiscale wavelet methods for PDEs*, pages 287–346, Academic Press, San Diego, 1997.
- [27] S. Sauter and C. Schwab. Quadrature for the hp -Galerkin BEM in \mathbb{R}^3 . *Numer. Math.*, 78:211–258, 1997.
- [28] R. Schneider. *Multiskalen- und Wavelet-Matrixkompression: Analysisbasierte Methoden zur Lösung großer vollbesetzter Gleichungssysteme*. B.G. Teubner, Stuttgart, 1998.
- [29] C. Schwab. Variable order composite quadrature of singular and nearly singular integrals. *Computing*, 53:173–194, 1994.
- [30] E.E. Tyrtyshnikov. Mosaic skeleton approximation. *Calcolo*, 33:47–57, 1996.
- [31] L. Villemoes. Wavelet analysis of refinement equations. *SIAM J. Math. Anal.*, 25:1433–1460, 1994.